

Water-Soluble Cationic Poly(*p*-phenyleneethynylene)s (PPEs): Effects of Acidity and Ionic Strength on Optical Behavior

Qu-Li Fan, Ying Zhou, Xiao-Mei Lu, Xiao-Yuan Hou, and Wei Huang\*

*Institute of Advanced Materials (IAM), Fudan University, 220 Handan Road, Shanghai 200433, The People's Republic of China**Received June 26, 2004; Revised Manuscript Received January 12, 2005*

**ABSTRACT:** Three cationic PPEs **P1'**–**P3'** were obtained through quaternization of their neutral polymers, of which all side chains were respectively featured with a tertiary amino group (**P1**), an alternative tertiary amino and tri(ethylene glycol)methyl ether group (**P2**), and an alternative tertiary amino and dodecyloxy group (**P3**). **P1'** showed intrinsic water-solubility although its quaternization degree was only 45%. Slightly blue-shifted UV–vis absorption maxima in an acidic environment (maximal  $\Delta\lambda_{\text{max}} \approx 3$  nm) and obvious red-shifted absorption (maximal  $\Delta\lambda_{\text{max}} \approx 30$  nm) and emission maxima (maximal  $\Delta\lambda_{\text{max}} \approx 20$  nm) in an alkaline environment at pH < 13 are explained in terms of pH-induced planarization of the conjugated backbone. After the pH was increased to 14, a new absorption ( $\lambda_{\text{max}} \approx 478$  nm) and emission ( $\lambda_{\text{max}} \approx 495$  nm) peak appeared in the redder region and the fluorescence intensity further dramatically decreased, implying the occurrence of the conformational change from the planarization of conjugated backbone to the interchain aggregation. The fluorescence enhancement of **P1'** in an acidic environment and the fluorescence decrease of **P1'** in an alkaline environment are attributed to the pH-influenced quenching ability of the nonbonding electron pair on the nitrogen atom, which belongs to the unquaternized tertiary amino group on the side chain, and the interchain aggregation. Such pH-influenced fluorescence intensity can be efficiently buffered by adding salts at pH < 10. Although adding salts in a neutral environment only creates the planarization of PPE conjugated backbone, adding salts in an alkaline environment significantly promotes the formation of interchain aggregation. Amplified quenching of **P1'** by anionic quencher  $\text{Fe}(\text{CN})_6^{4-}$  was observed and its  $K_{\text{sv}}$  increased significantly after adding salts or increasing pH to 14, for example from  $K_{\text{sv}} = 9.6 \times 10^5 \text{ M}^{-1}$  at pH = 7 to  $7.7 \times 10^6 \text{ M}^{-1}$  at pH = 10 when  $[\text{NaCl}] = 0.1 \text{ M}$ , due to the formation of elongated  $\pi$ -conjugation.

## Introduction

In the past few years, fluorescent water-soluble conjugated polymers (FWSCPs) containing charged groups have showed great potential as novel chemo or biosensors due to their amplified fluorescence quenching ability upon electron or energy transfer by quenchers with counterions.<sup>1,2</sup> To develop FWSCPs as practical sensors, the optophysical properties of FWSCPs in different aqueous environments were studied intensively and they showed that their optical properties and quenching behavior varied in accordance with the change of local environments, such as ionic strength,<sup>3</sup> charge on quencher,<sup>4</sup> concentration of surfactant<sup>5,6</sup> or polyelectrolyte<sup>7,8</sup> with counterions, and type of substrate.<sup>7</sup> Most of the above investigations were performed in a neutral environment. In practice, analysis in the environments with different pH is nearly inevitable, while the related pH-influenced analytical efficiency is seldom reported.<sup>9</sup> Although Pinto and Schanze recently studied the optical properties of an anionic poly(*p*-phenyleneethynylene) (PPE) in an alkaline environment and reported its interchain aggregation with pH decrease,<sup>10</sup> investigation of the influence of pH and its combination with other factors, e.g., ionic strength) on the conformational change and the related optical behavior of FWSCPs in both acidic and alkaline environments is more significant and exigent to develop FWSCPs as good biosensors in a wider scope.

Anionic FWSCPs are a versatile class of polyelectrolytes which can be easily fabricated through grafting different types of anionic groups (sulfonated, carboxylic and phosphonated group) to the side chains of conjugated polymers with various backbones.<sup>11</sup> Since a water-soluble sulfonated poly(phenylenevinylene) (PPV– $\text{SO}_3^-$ ) was first used by Chen et al. to detect proteins,<sup>1</sup> anionic FWSCPs have been the subject of intensive studies on their application as biosensors.<sup>12</sup> Their optophysical properties in an aqueous solution were highly investigated.<sup>3–8,13,14</sup> Compared with anionic FWSCPs, cationic FWSCPs attracted little attention previously because of no report on them as biosensors and their relatively fewer types (cationic groups are mostly ammonium groups).<sup>11</sup> In 1999, Schanze and Reynolds first reported the amplified fluorescence quenching in a poly(*p*-phenylene)-based cationic polyelectrolyte.<sup>15</sup> Most recently, cationic ammonium-functionalized polyfluorene (PF– $\text{NEt}_3^+$ ) was successfully developed to identify specific anionic DNA<sup>2,16</sup> and a major effort is being focused on determining the relationship between polyfluorene chemical structure and its corresponding biosensitivity.<sup>17–19</sup> The novel application of cationic FWSPs encouraged us to develop additional cationic FWSCP types and investigate their optophysical properties in an aqueous solution.

PPE is a kind of conjugated polymer which is suitable to study optical property-structure relationship because of its good optical response on environmental variation through the relatively free rotation of alkyne–aryl single bond and interchain aggregation.<sup>20</sup> In addition, because of the high delocalization of singlet exciton in PPEs and the rapidness of the energy migration along

\* To whom correspondence should be addressed. Telephone: +86 (21) 5566 4188. Fax: +86 (21) 6565 5123. E-mail: wei-huang@fudan.edu.cn/iamdirector@fudan.edu.cn.

the conjugated backbone, PPEs used as chemosensors in organic solvent and as films have been widely reported by Swager et al.<sup>21</sup> Currently, the preparation of water-soluble PPEs and the study on their optical properties in aqueous solution have attracted much attention to fabricate novel chemo or biosensors. In such, different types of anionic water-soluble PPEs were widely investigated.<sup>10,22–25</sup> However, for cationic PPEs, as far as we know, only Swager et al. reported its application in layer-by-layer self-assembling ultrathin film through electrostatic attraction.<sup>26</sup>

Herein, we report the successful synthesis of a neutral PPE with quaternizable tertiary amino groups on all side chains. Quaternization after polymerization was chosen to obtain a new cationic water-soluble conjugated polyelectrolyte. In an attempt to develop intrinsically water-soluble PPE polyelectrolytes, tertiary amino group (the quaternizable group) was introduced into all side chains of the neutral conjugated polymer instead of one moiety of the side chains<sup>26</sup> and expected to enhance the charge density on the conjugated polyelectrolyte by quaternization. The other two cationic PPE polymers containing side chains with different hydrophilicity respectively were also synthesized and the water solubility of the three cationic PPEs was compared with each other. The pH- and ionic-strength-influenced conformational change and the related optical behavior of the new water-soluble PPE were intensively investigated in both acidic and alkaline environments (pH = 2–14).

## Experimental Section

**General Methods.** The NMR spectra were collected on a Varian Mercury Plus 400 spectrometer with tetramethylsilane as the internal standard. FT-IR spectra were recorded on a Shimadzu IRPrestige-21 FTIR-8400s spectrophotometer by dispersing samples in KBr. Mass spectra (MS) were obtained using a HP 5973MS mass spectrometer at an ionizing voltage of 70 eV. UV–vis spectra were recorded on a Shimadzu 3150 PC spectrophotometer. The concentrations of copolymer solutions were adjusted to about 0.01 mg/mL or less. Fluorescence measurement was carried out on a Shimadzu RF-5301 PC spectrofluorophotometer with a xenon lamp as a light source. Thermogravimetric analysis (TGA) was performed on a Shimadzu thermogravimetry and differential thermal analysis DTG-60H at a heating rate of 10 °C/min under N<sub>2</sub>. Elemental microanalyses were carried out on a Vario EL III CHNOS Elemental analyzer. Gel permeation chromatography (GPC) analysis was conducted with a HP1100 HPLC system equipped with 7911GP-502 and GP NXC columns using polystyrenes as the standard and tetrahydrofuran (THF) as the eluant at a flow rate of 1.0 mL/min and 35 °C. Time-correlated single photon fluorescence studies were performed using an Edinburgh Instruments LifeSpec-PS spectrometer. The LifeSpec-PS comprises a 371 nm picosecond laser (PicoQuant PDL 800B) operated at 2.5 MHz and a Peltier-cooled Hammamatsu microchannel plate photomultiplier (R3809U-50). Lifetimes were determined from the data using the Edinburgh Instruments software package.

The pH-dependent electronic spectra were investigated in polymer aqueous solution (5  $\mu$ M) in which the pH was varied from 2 to 12. The quenching behavior was studied by comparing the fluorescence intensities of polymer aqueous solutions in the presence of quenchers with different concentrations. Milli-Q water used in preparing the aqueous solutions of the polymers and quenchers was purged with nitrogen for 4 h before using.

**Materials.** All chemical reagents used were purchased from Aldrich Chemical Co. THF was purified by distillation from sodium in the presence of benzophenone. Toluene was purified by distillation from sodium. Other organic solvents were used without any further purification. 2,5-Diiodo-1,4-bis(dodecyl-

oxy)benzene, 1,4-diiodo-2,5-bis{2-[2-(2-methoxyethoxy)ethoxy]ethoxy}benzene, and 1,4-diiodo-2,5-hydroquinone were synthesized according to the literature procedures.<sup>20,21b,27</sup>

**Synthesis. 1,4-Bis[3-(*N,N*-diethylamino)-1-oxapropyl]-2,5-diiodobenzene (Monomer 1).** A 250 mL round-bottom flask with magnetic stirring bar was charged with anhydrous potassium carbonate (24.84 g, 0.18 mol), 1,4-diiodo-2,5-hydroquinone (10.86 g, 0.03 mol), and 150 mL of acetone. The stirred mixture was sparged with nitrogen for 15 min and then refluxed for about 30 min. After 30 min of refluxing, 2-chlorotriethylamine hydrochloride (12.38 g, 0.072 mol) was added into the round-bottom flask and the mixture was then refluxed for 3 days. The precipitate mixture was filtered away, and the filtrate was rotary evaporated. The residue was poured into water and extracted with ether three times, and the combined organics were washed with 10% aqueous sodium hydroxide twice, water twice, and brine once. The solution was dried over magnesium sulfate, filtered and stripped off solvent by rotary evaporation to yield crude solid. The crude product was recrystallized with hexane to afford colorless crystals (12 g, yield 71%). Mp: 76–78 °C. MS:  $m/z$  559.9. <sup>1</sup>H NMR (CDCl<sub>3</sub>, ppm):  $\delta$  7.23 (s, 2 H), 4.02 (t, 4 H,  $J$  = 6.4 Hz), 2.93 (t, 4 H,  $J$  = 6.4 Hz), 2.67 (q, 8 H,  $J$  = 6.4 Hz), 1.10 (t, 12 H,  $J$  = 6.8 Hz). <sup>13</sup>C NMR (CDCl<sub>3</sub>, ppm):  $\delta$  153.4, 123.4, 86.5, 69.8, 52.0, 48.4, 12.6. Anal. Calcd for C<sub>18</sub>H<sub>30</sub>I<sub>2</sub>N<sub>2</sub>O<sub>2</sub>: C, 38.59; H, 5.40; N, 5.00; I, 45.30. Found: C, 38.99; H, 5.32; N, 4.84.

**1,4-Diethynyl-2,5-bis[3-(*N,N*-diethylamino)-1-oxapropyl]benzene (Monomer 2).** A 4.66 g (0.01 mol) sample of monomer 1, 0.35 g (0.5 mmol) of PdCl<sub>2</sub>(PPh<sub>3</sub>)<sub>2</sub> and 0.0952 g (0.5 mmol) of CuI were dissolved in 40 mL of diisopropylamine. 2.156 g (0.022 mol) of (trimethylsilyl)acetylene was added into the vigorously stirred solution at room temperature under nitrogen protection. After the addition was finished, the reaction mixture was stirred at reflux for 3 h. After the solvent was evaporated under reduced pressure, the residue was poured into 100 mL of water and extracted with chloroform three times. The combined organic layer was washed with water twice and brine once and dried over MgSO<sub>4</sub>. After the mixture was filtered, 5 mL of hydrazine monohydrate dissolved in 10 mL of water was poured into the filtrate and stirred vigorously for 12 h. The organic layer was separated and washed with water three times and brine once and dried over MgSO<sub>4</sub>. After the solvent was evaporated, the residue was dissolved in a mixture of KOH (1 g in 2 mL of water) and 100 mL of methanol and stirred at room temperature for 1 h. After evaporation of the solvent, the mixture was subjected to a CHCl<sub>3</sub>/H<sub>2</sub>O workup. The organic phases were combined and dried over MgSO<sub>4</sub>. The solvent was removed under reduced pressure, and the deep black residue was added into 100 mL of saturated HCl methanol solution and stirred for 30 min at room temperature. The solvent was evaporated and the crude product was recrystallized with ethanol to afford light yellow crystals (3.1 g, yield 72%). Mp: 230–1 °C. <sup>1</sup>H NMR (D<sub>2</sub>O, ppm):  $\delta$  7.17 (s, 2 H), 4.34 (t, 4 H,  $J$  = 5.2 Hz), 3.84 (s, 2 H), 3.58 (t, 4 H,  $J$  = 4.8 Hz), 3.32 (q, 8 H,  $J$  = 7.2 Hz), 1.28 (t, 12 H,  $J$  = 7.2 Hz).

The abovementioned compound was dissolved in 50 mL of water and K<sub>2</sub>CO<sub>3</sub> aqueous solution (3 g in 50 mL water) was added dropwise at room temperature and stirred for 30 min. After the stirring, the obtained light yellow organic layer was separated and the water layer was extracted with chloroform three times. The combined organic layers were washed with water twice and brine once and dried over MgSO<sub>4</sub>. The mixture was filtered, and the filtrate was evaporated using rotary evaporator to afford yellow crystals (2.49 g, yield 97%). Mp: 70–1 °C. MS:  $m/z$  356.2. <sup>1</sup>H NMR (CDCl<sub>3</sub>, ppm):  $\delta$  6.99 (s, 2 H), 4.07 (t, 4 H,  $J$  = 6.0 Hz), 3.34 (s, 2 H), 2.93 (t, 4 H,  $J$  = 6.0 Hz), 2.66 (q, 8 H,  $J$  = 7.2 Hz), 1.09 (t, 12 H,  $J$  = 7.2 Hz). <sup>13</sup>C NMR (CDCl<sub>3</sub>, ppm):  $\delta$  154.4, 118.0, 113.6, 83.0, 80.1, 68.7, 51.9, 48.3, 12.4. Anal. Calcd for C<sub>22</sub>H<sub>32</sub>N<sub>2</sub>O<sub>2</sub>: C, 74.12; H, 9.05; N, 7.86. Found: C, 74.05; H, 8.99; N, 7.73.

**1,4-Diphenylethynyl-2,5-bis[3-(*N,N*-diethylamino)-1-oxapropyl]benzene (M1).** First, 2.8 g (0.005 mol) sample of monomer 1, 0.29 g (0.25 mmol) of Pd(PPh<sub>3</sub>)<sub>4</sub>, and 0.19 g (0.001 mol) CuI were dissolved in 15 mL of diisopropylamine. Then



1.12 g (0.011 mol) of phenylacetylene was added into the vigorously stirred solution at room temperature under nitrogen protection. After the addition was finished, the reaction mixture was stirred at reflux for 12 h. The purification procedure of monomer **2** was followed to obtain 1,4-Diphenylethynyl-2,5-bis[3-(*N,N*-diethylamino)-1-oxapropyl]benzene as white crystals (1.81 g, yield 71%).  $^1\text{H}$  NMR ( $\text{CDCl}_3$ , ppm):  $\delta$  7.51 (m, 4 H), 7.37 (m, 6 H), 7.09 (s, 2 H), 4.11 (t, 4 H,  $J = 5.2$  Hz), 2.94 (t, 4 H,  $J = 5.2$  Hz), 2.69 (q, 8 H,  $J = 7.2$  Hz), 1.05 (t, 2 H,  $J = 7.2$  Hz).  $^{13}\text{C}$  NMR ( $\text{CDCl}_3$ , ppm):  $\delta$  153.6, 131.3, 128.4, 123.5, 116.6, 114.0, 94.6, 85.7, 67.8, 51.2, 10.6.

**1,4-Diphenylethynyl-2,5-bis[3-(*N,N,N*-triethylammonium)-1-oxapropyl]benzene Dibromide (M1').** First 1.02 g (0.002 mol) of **M1** was dissolved in 40 mL THF, and then 10 mL bromoethane was added into the solution under nitrogen protection. The mixture was stirred with refluxing for 5 days and then filtered to get the crude product. The crude product was recrystallized with ethanol to afford pure light yellow crystals (0.95 g, yield 65%).  $^1\text{H}$  NMR ( $\text{CD}_3\text{OD}$ , ppm):  $\delta$  7.53 (m, 4 H), 7.42 (m, 6 H), 7.32 (s, 2 H), 4.50 (m, 4 H,  $J = 4.2$  Hz), 3.83 (t, 4 H,  $J = 4.2$  Hz), 3.52 (q, 12 H,  $J = 7.2$  Hz), 1.07 (t, 18 H,  $J = 7.2$  Hz).  $^{13}\text{C}$  NMR ( $\text{CD}_3\text{OD}$ , ppm):  $\delta$  154.0, 132.6, 130.1, 129.8, 124.1, 118.4, 115.2, 96.3, 86.2, 64.1, 57.1, 55.0, 8.1.

**General Procedure for the Preparation of P1, P2, and P3.** Under argon protection, diisopropylamine/toluene (3:7, 35 mL) was added to a 50 mL round-bottom flask containing a 0.272 g (0.765 mmol) sample of monomer **2**, 0.75 mmol of diiodobenzene monomer (0.420 g of monomer **1**, 0.491 g of 1,4-diiodo-2,5-bis[2-[2-(2-methoxyethoxy)ethoxy]ethoxy]benzene or 0.524 g of 2,5-diiodo-1,4-bis(dodecyloxy)benzene), 51.9 mg (0.045 mmol) of  $\text{Pd}(\text{PPh}_3)_4$ , and 42.8 mg (0.225 mmol) of CuI. The mixture was heated at 70 °C for 24 h and then subjected to a  $\text{CHCl}_3/\text{H}_2\text{O}$  workup. The combined organic phase was washed with water  $\text{NH}_4\text{OH}$  (50%) twice, water twice, and brine once and dried over  $\text{MgSO}_4$ . The solution was removed in vacuo, and the residue was redissolved in 10 mL of  $\text{CHCl}_3$  and reprecipitated in methanol twice. The mixture was filtered to afford a yellow solid.

**P1:** 0.42 g (yield 85%).  $^1\text{H}$  NMR ( $\text{CDCl}_3$ , ppm):  $\delta$  7.04 (s, 2 H), 4.12 (t, 4 H), 2.95 (t, 4 H), 2.70 (q, 8 H), 1.08 (t, 12 H).  $^{13}\text{C}$  NMR ( $\text{CDCl}_3$ , ppm):  $\delta$  153.8, 117.5, 114.6, 91.9, 68.8, 52.1, 48.4, 12.6. FT-IR (KBr pellet,  $\text{cm}^{-1}$ ): 3429 (br), 3055, 2967, 2930, 2872, 2816, 2199, 1512, 1464, 1426, 1379, 1275, 1211, 1042, 953, 860, 802, 740, 717, 510. Anal. Calcd for  $\text{C}_{20}\text{H}_{30}\text{N}_2\text{O}_2$ : C, 72.69; H, 9.15; N, 8.48. Found: C, 71.95; H, 8.68; N, 8.04.

**P2:** 0.46 g (yield 81%).  $^1\text{H}$  NMR ( $\text{CDCl}_3$ , ppm):  $\delta$  7.07 (s, 2 H), 7.04 (s, 2 H), 4.24 (br, 4 H), 4.15 (br, 4 H), 3.93 (br, 4 H), 3.80 (br, 4 H), 3.65 (br, 8 H), 3.53 (br, 4 H), 3.36 (s, 6 H), 2.99 (br, 4 H), 2.71 (br, 8 H), 1.09 (t, 12 H).  $^{13}\text{C}$  NMR ( $\text{CDCl}_3$ , ppm):  $\delta$  153.8, 118.1, 117.5, 114.9, 114.6, 92.0, 72.1, 71.7, 71.2, 71.0, 70.5, 70.3, 68.8, 52.0, 48.4, 12.6. FT-IR (KBr pellet,  $\text{cm}^{-1}$ ): 3483 (br), 3056, 2967, 2929, 2873, 2816, 2200, 1510, 1456, 1425, 1372, 1277, 1218, 1107, 1042, 953, 858, 803, 741, 717, 512. Anal. Calcd for  $\text{C}_{42}\text{H}_{62}\text{N}_2\text{O}_{10}$ : C, 66.82; H, 8.28; N, 3.71. Found: C, 64.15; H, 7.90; N, 3.28.

**P3:** 0.48 g (yield 80%).  $^1\text{H}$  NMR ( $\text{CDCl}_3$ , ppm):  $\delta$  7.06 (s, 2 H), 7.03 (s, 2 H), 4.14 (br, 4 H), 4.05 (br, 4 H), 2.99 (br, 4 H), 2.70 (q, 8 H), 1.88 (br, 4 H), 1.52 (br, 4 H), 1.43–1.22 (br, 32 H), 1.09 (t, 12 H), 0.89 (t, 6 H).  $^{13}\text{C}$  NMR ( $\text{CDCl}_3$ , ppm):  $\delta$  153.7, 117.5, 114.6, 91.9, 70.0, 68.8, 51.9, 48.3, 32.0, 29.8, 29.7, 29.5, 29.4, 26.0, 22.7, 14.1, 12.2. FT-IR (KBr pellet,  $\text{cm}^{-1}$ ): 3446 (br), 3057, 2964, 2924, 2868, 2815, 2200, 1510, 1463, 1428, 1386, 1278, 1213, 1043, 955, 861, 804, 740, 721, 511. Anal. Calcd for  $\text{C}_{52}\text{H}_{82}\text{N}_2\text{O}_4$ : C, 78.15; H, 10.34; N, 3.51. Found: C, 76.64; H, 9.80; N, 3.08.

**General Procedure for the Preparation of P1', P2', and P3' via Quaternization of the Neutral Polymers (P1, P2, and P3, Respectively).** A 50 mL round-bottom flask with a magnetic spin bar was charged with 1 mmol (based on repeat unit) of neutral polymer (0.330 g of **P1**, 0.378 g of **P2**, or 0.400 g of **P3**). The polymer was dissolved in 20 mL of THF. To this was added bromoethane (1.09 g, 10 mmol) and 5 mL of DMSO. The solution was stirred at 50 °C for 5 days. **P1':** During the

quaternization, a yellow precipitate was produced in the solution. The resulting precipitate was collected on a frit at reduced pressure and dried to get 0.41 g of the desired product (yield 75%).  $^1\text{H}$  NMR ( $\text{D}_2\text{O}$ , ppm):  $\delta$  7.26 (br, 2 H), 4.44 (br, 4 H), 3.73 (br, 1.8 H), 3.60 (br, 2.2 H), 3.40 (br, 4.3 H), 3.31 (br, 5.4 H), 1.20 (br, 12 H).  $^{13}\text{C}$  NMR ( $\text{D}_2\text{O}$ , ppm):  $\delta$  153.3, 117.6, 114.1, 91.4, 64.8, 63.6, 58.5, 56.0, 54.3, 51.4, 49.5, 9.1, 7.6. FT-IR (KBr pellet,  $\text{cm}^{-1}$ ): 3458 (br), 3056, 2970, 2947, 2870, 2659, 2484, 2202, 1510, 1467, 1422, 1397, 1275, 1216, 1059, 1020, 951, 864, 785, 715, 520. Anal. Calcd for  $\text{C}_{20}\text{H}_{30}\text{N}_2\text{O}_2 \cdot 0.9\text{C}_2\text{H}_5\text{Br} \cdot 0.5\text{H}_2\text{O}$ : C, 59.84; H, 8.18; N, 6.40; Br, 16.44. Found: C, 58.04; H, 7.35; N, 5.55; Br, 17.87. The water present in the elemental analysis results was based on mass loss in the TGA and the bromide determination was carried out by Schöniger combustion method and then titration with  $\text{HgNO}_3$ .

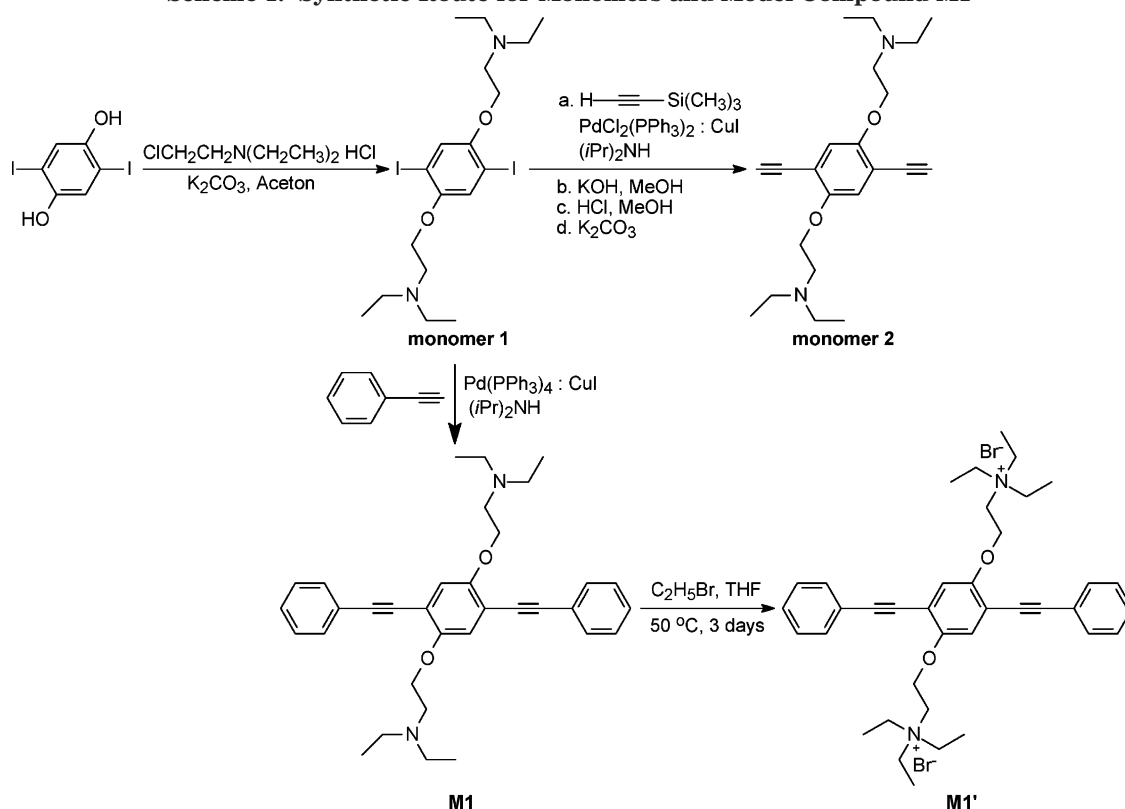
**P2':** Most of the bromoethane and THF was evaporated and then the quaternized polymer was precipitated in 100 mL of acetone, collected by centrifugation and dried overnight in vacuo at 50 °C (0.345 g, yield 71%).  $^1\text{H}$  NMR ( $\text{CD}_3\text{OD}$ , ppm):  $\delta$  7.37 (br, 2 H), 7.27 (br, 2 H), 4.57 (br, 4 H), 4.29 (br, 4 H), 3.94 (br), 3.78 (br), 3.63 (br), 3.52 (br), 3.35 (br), 1.37 (br, 17.1 H).  $^{13}\text{C}$  NMR ( $\text{CD}_3\text{OD}$ , ppm):  $\delta$  153.3, 152.7, 118.1, 117.9, 114.3, 92.3, 91.4, 72.5, 71.5, 71.0, 69.7, 64.8, 63.6, 60.0, 58.6, 56.2, 54.2, 51.8, 49.5, 9.2, 7.4. FT-IR (KBr pellet,  $\text{cm}^{-1}$ ): 3430 (br), 3056, 2980, 2932, 2880, 2650, 2483, 2203, 1508, 1464, 1423, 1398, 1275, 1218, 1097, 1052, 1026, 949, 852, 790, 716, 527. Anal. Calcd for  $\text{C}_{42}\text{H}_{62}\text{N}_2\text{O}_{10} \cdot 1.7\text{C}_2\text{H}_5\text{Br} \cdot \text{H}_2\text{O}$ : C, 56.91; H, 7.63; N, 2.92; Br, 14.18. Found: C, 58.77; H, 7.75; N, 2.67; Br, 15.50.

**P3':** Most of the bromoethane and THF was evaporated and then the quaternized polymer was precipitated in 100 mL of acetone, collected by centrifugation and dried overnight in vacuo at 50 °C (0.392 g, yield 77%).  $^1\text{H}$  NMR ( $\text{CD}_3\text{OD}$ , ppm):  $\delta$  7.34 (br, 2 H), 7.19 (br, 2 H), 4.54 (br, 4 H), 4.12 (br, 4 H), 3.74 (br, 4 H), 3.51 (br, 11.8 H), 1.85 (br, 4 H), 1.57 (br, 4 H), 1.37 (br), 1.27 (br), 0.89 (br, 6 H).  $^{13}\text{C}$  NMR ( $\text{CD}_3\text{OD}$ , ppm):  $\delta$  154.2, 153.3, 117.8, 114.9, 91.2, 70.3, 64.8, 54.3, 51.3, 49.3, 32.1, 29.8, 29.6, 26.3, 22.8, 13.5, 8.7, 7.2. FT-IR (KBr pellet,  $\text{cm}^{-1}$ ): 3420 (br), 3056, 2968, 2924, 2853, 2627, 2475, 2203, 1510, 1467, 1422, 1392, 1271, 1214, 1057, 1020, 947, 863, 798, 718, 517. Anal. Calcd for  $\text{C}_{52}\text{H}_{82}\text{N}_2\text{O}_4 \cdot 1.9\text{C}_2\text{H}_5\text{Br} \cdot 2.5\text{H}_2\text{O}$ : C, 63.75; H, 9.25; N, 2.66; Br, 14.44. Found: C, 61.68; H, 8.47; N, 2.78; Br, 14.92.

## Results and Discussion

**Synthesis of Monomers and Polymers.** The preparation of monomers is shown in Scheme 1. 2,5-Bis[3-(*N,N*-diethylamino)-1-oxapropyl]-1,4-diiodobenzene (monomer **1**) was prepared from 2,5-diiodohydroquinone by a reaction with 2-(diethylamino)ethyl chloride hydrochloride in refluxing acetone in the presence of excess anhydrous potassium carbonate. Consequently, treating monomer **1** with trimethylsilyl acetylene afforded di(trimethylsilyl)ethynyl compounds which was further converted to the key monomer **2** under base treatment. Syntheses of the polymers are outlined in Scheme 2. The preparation of neutral polymers **P1**–**P3** was accomplished via Sonogashira reaction of corresponding monomers with key monomer **2** in the mixture of toluene and diisopropylamine solution in the presence of  $\text{Pd}(\text{PPh}_3)_4/\text{CuI}$  catalyst at 70 °C for 1 day. Conversion of the neutral polymers to the final cationic polymers was achieved by treating **P1**–**P3** with bromoethane in the mixture of DMSO and THF (1:4) at 50 °C for 5 days. In contrast to the direct synthesis of cationic PPE by Swager et al.,<sup>26</sup> quaternization after polymerization was adopted to obtain cationic PPEs in our present work because those neutral analogues can be purified and analyzed by a conventional method.<sup>28,29</sup> Furthermore, the tunable quaternization degree of cationic PPEs obtained by quaternization after polym-

Scheme 1. Synthetic Route for Monomers and Model Compound M1'



erization makes them attractive for applications in organic LEDs and as fluorescence biosensors through layer-by-layer self-assembly.<sup>30</sup> Gel permeation chromatography reveals that all of the neutral polymers showed reasonably high molecular weight (see Table 1). Thermogravimetric analysis (see Figure 1) shows  $T_d$  at nearly  $200^\circ\text{C}$  of those quaternized polymers made them enough serve as chemo- or biosensor because all of applications proceed at room temperature.

To compare the effect of hydrophilicity of the side chains on water solubility of the polymers, dodecyloxy or tri(ethylene glycol)methyl ether groups were also employed, as our group previously adopted in the cationic PPV system.<sup>31</sup> All the neutral polymers **P1**–**P3** were readily soluble in common organic solvents such as chloroform and THF but insoluble in methanol, DMSO and DMF. **P1'** and **P2'** exhibited good solubility in both methanol and water, while **P3'** could be dissolved in methanol but not water due to the existence of long hydrophobic side chains.<sup>31</sup>

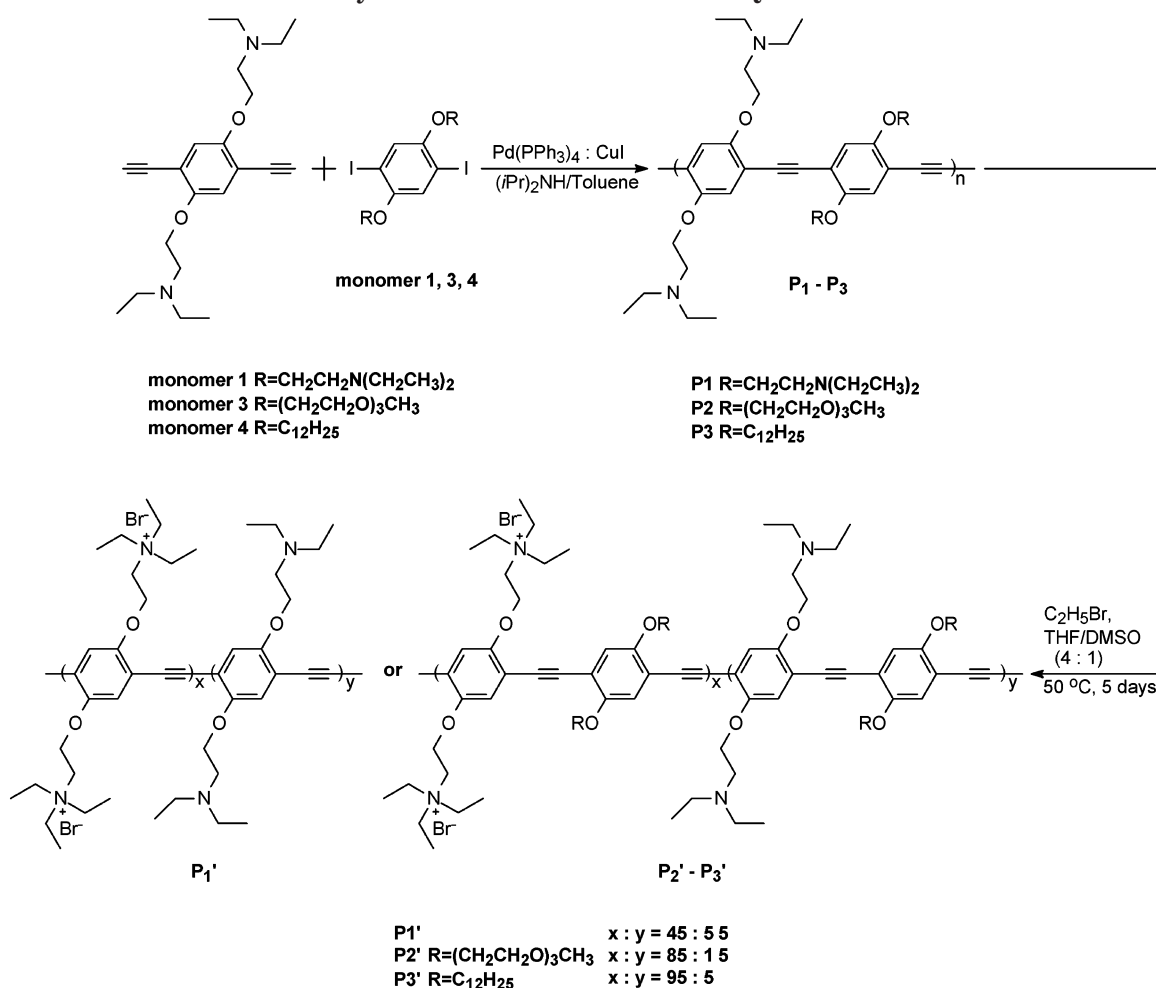
The quaternization degrees (QDs) of **P1'**–**P3'** could be determined by  $^1\text{H}$  NMR spectra. As shown in Figure 2, the neutral polymer **P1** exhibited two well-resolved peaks at 2.95, and 2.70 ppm corresponding to the methylene groups adjacent to the nitrogen ( $-\text{CH}_2\text{N}-$ ) atoms. After the treatment with bromoethane, all signals corresponding to  $-\text{CH}_2\text{N}-$  split into two peaks, which arise from the quaternized (low field) and unquaternized components.<sup>29,30</sup> The relative integrals of each pair of the split peaks can thus be used to estimate the QD of **P1'** which was 45%. However, for **P2'** and **P3'**, the QD of **P2'** (85%) was determined by the relative integrals of the methylene ( $-\text{NCH}_2\text{CH}_2\text{O}-$ ) and methyl ( $-\text{NCH}_2\text{CH}_3$ ) peaks and that of **P3'** (95%) was calculated from the relative integrals of the methylene (in  $-\text{OCH}_2\text{CH}_2\text{N}-$ ) and methylene (in  $-\text{NCH}_2\text{CH}_3$ ) peaks. The higher QDs of **P2'** and **P3'** than that of **P1'**,

combined with the fact that **P1'** precipitated while **P2'** and **P3'** showed good solubility during their quaternization process, indicated that, under the same quaternization conditions, the existence of longer side chains may be more beneficial to the completion of the quaternization. It is noteworthy that although the quaternization degree of **P1'** is only 45%, much lower than what we expected,  $^1\text{H}$  NMR measurement showed that water is a better solvent for **P1'** than for **P2'** and other reported cationic PPE derivatives with similar structure<sup>26</sup> as **P2'**, indicating clearly that introducing more percentage of tertiary amino groups into the side chains of neutral PPE is very efficient to obtain cationic PPE with intrinsic water solubility.

**General Optical Properties.** The UV–vis and photoluminescence spectra of the neutral polymers in  $\text{CHCl}_3$  are shown in Figure 3a. **P1**–**P3** exhibited a strong absorption peak occurring at 433, 430, and 444 nm respectively, while all the emission peaks of **P1**–**P3** appeared at about 472 nm with a vibronic band shoulder at 506 nm. All absorption and emission spectra were almost identical to what Wrighton et al. reported previously,<sup>32</sup> indicating that the electronic properties of these conjugated polymers were predominantly governed by the rigid-rod and highly conjugated polymer backbone and ancillary influenced by the nature of the attached side chains.

Figure 3b shows the UV–vis and photoluminescence spectra of the quaternized polymers in  $\text{CH}_3\text{OH}$  and water. In comparison with that of the neutral polymers, the absorption and emission peaks of all quaternized polymers present obvious blue-shift (detailed data please see Table 1). This is resulted from the mutual repulsion among the positive charges leading to a more twisted main chain conformation, and hence a decreased effective conjugation length.<sup>28–31</sup> Meanwhile, the absorption and emission maxima of those quaternized polymers are

Scheme 2. Synthetic Routes for Neutral and Quaternized PPEs

Table 1. Characterization of Neutral Polymers and Quaternized Polymers<sup>a</sup>

polymer	GPC			absorption $\lambda_{\text{max}}/\text{nm}$			emission $\lambda_{\text{max}}/\text{nm}$		
	$M_n$	$M_w$	PDI	$\text{CHCl}_3$	$\text{CH}_3\text{OH}$	$\text{H}_2\text{O}$	$\text{CHCl}_3$	$\text{CH}_3\text{OH}$	$\text{H}_2\text{O}$
P1	26 700	61 200	2.29	433			471		
P2	20 300	46 700	2.30	430			470		
P3	47 100	138 800	2.95	444			474		
P1'					403	378		457	444
P2'					416	404		463	457
P3'					426, 480			466, 496	

<sup>a</sup>  $M_n$ ,  $M_w$ , and PDI of the polymers were determined by gel permeation chromatography using polystyrene standards.

remarkably dependent on the solvent, showing an obvious bathochromic shift with the decrease of solvent polarity. Interestingly, a new absorption maximum was observed at about 480 nm for **P3'**. Note that **P3'** has an alternatively hydrophilic–hydrophobic side chain pattern, the conjugated segments may have a strong tendency to form interchain aggregates.<sup>22</sup> An aggregation absorption at about 470 nm was previously observed by Swager et al. in investigating the LB films of a series of PPE derivatives, which is quite close to the value in our system.<sup>33</sup> In addition, the formation of interchain aggregation can be further evidenced by the fact that such a new absorption peak could disappear thoroughly by adding THF (good solvent for those hydrophobic groups) while showed no response to the introduction of water (good solvent for those hydrophilic groups). The abovementioned results strongly support our previous conclusion that increasing the percentage

of hydrophilic groups is beneficial to improving the water-solubility of conjugated polymers.

**pH-Influenced UV–Vis Absorption and Photoluminescence of P1'.** It was found that the yellow color of **P1'** aqueous solution changed into light color when adding HCl aqueous solution while turned into deep yellow color after adding NaOH aqueous solution. This color tunability was similar to that of water-soluble anionic polythiophene by changing the counteranion,<sup>34</sup> indicating the obvious pH-induced variation of UV–vis absorption for **P1'**.

Figure 4a shows the UV–vis absorption of **P1'** aqueous solution with different pH. As shown in Figure 4a, the absorption maximum was slightly blue-shifted when  $\text{pH} < 7.0$ , indicating the formation of a less effective conjugated length in the backbone. Because of the existence of unquaternized amino groups (55%) in **P1'**, adding acid was considered to acidify those unquater-

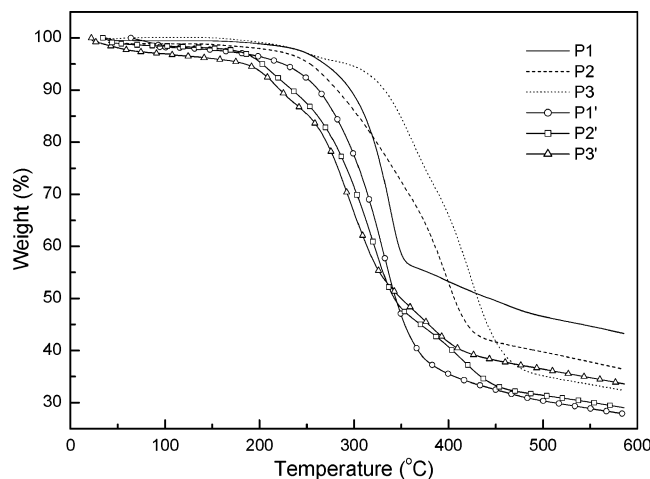


**Figure 1.** Thermalgravimetric analyses of the neutral and quaternized PPEs.

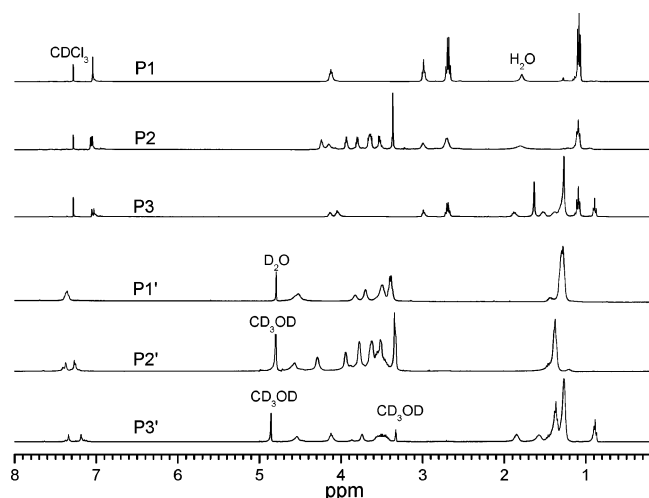


**Figure 2.**  $^1\text{H}$  NMR spectra of neutral polymers **P1**–**P3** in  $\text{CDCl}_3$  and quaternized polymers **P1'** in  $\text{D}_2\text{O}$  and **P2'**–**P3'** in  $\text{CD}_3\text{OD}$ .

nized amino groups into cationic ammonium groups and thus enhance the strong electrostatic repulsion among the positive charges which resulted in the more torsional angle of the conjugated backbone.<sup>28–31</sup> The increased torsional structure due to the free internal rotation of alkyne-aryl single bond shortened the efficient  $\pi$ – $\pi$  conjugation system of PPE, and led to a blue-shift of absorption maximum.

After dropping NaOH aqueous solution (0.1 M) into **P1'** solution at a high concentration (0.01 M), the **P1'** solution color initially changed into deep yellow color, and then an orange solid was precipitated from **P1'** solution. To clarify if such a precipitate resulted from the destruction of the chemical structure of **P1'** under an alkaline environment, the HCl solution was added to neutralize NaOH solution. It was showed that after being neutralized by HCl solution, the precipitate disappeared and was redissolved in aqueous solution. With the nonchanged NMR spectra of **P1'** after such a treatment, it can be demonstrated that **P1'** is not damaged by NaOH. Thus, the precipitate with pH increase can be attributed to the formation of aggregation.<sup>10</sup> Furthermore, we found that upon dropping NaOH aqueous solution into **P1'** solution at a much lower concentration (5  $\mu\text{M}$ ), a deeper color of **P1'** solution also became visible but no precipitate appeared. In

addition, the absorption maximum of **P1'** red-shifted obviously but no new absorption maximum appeared in redder region in an alkaline environment at pH < 13. However, when pH increased to 14, a new absorption peak appeared ( $\lambda_{\text{max}} = 476 \text{ nm}$ ) after the initial absorption maximum ended its red shift at  $\lambda_{\text{max}} = 408 \text{ nm}$ , indicating that the interchain aggregation was formed. This phenomenon suggests that the planarization of **P1'** conjugated backbone exist before its formation of interchain aggregation with pH increase, which is different from the results reported earlier where the formation of interchain aggregation for PPE– $\text{SO}_3^-$  with pH decrease was the only origin of the spectra shift.<sup>10</sup>

The investigation of the pH-influence on emission maxima of **P1'** further demonstrated the above conclusion. In Figure 4b, emission maximum little shifted in an acidic environment while red-shifted gradually in an alkaline environment. Combined with the gradual red-shift without the formation of a new absorption and emission peak, the maximal emission  $\Delta\lambda_{\text{max}} \approx 20 \text{ nm}$  in an alkaline environment at pH < 13 which is similar to the red shift of the PPE model compound by planarization<sup>35</sup> whereas lower than the reported red-shift (> 70 nm) of anionic PPE– $\text{PO}_3^-$  from interchain aggregation<sup>10,22</sup> strongly evidenced the formation of planarization of the conjugated backbone, not interchain aggregation. Time-resolved photoluminescent measurement excited at 380 nm in **P1'** aqueous solution with different pH (see Table 2) revealed a rapid monoexponential decay and no long-lived fluorescence (< 1 ns, due to interchain aggregation).<sup>10,22</sup> This further confirmed the nonexistence of interchain aggregation in an alkaline environment at pH < 13. When pH increased to 14, a new emission peak ( $\lambda_{\text{max}} = 494 \text{ nm}$ ,  $\Delta\lambda_{\text{max}} \approx 50 \text{ nm}$ ) and another long-lived fluorescence ( $\approx 6 \text{ ns}$ ) appeared, indicating the formation of interchain aggregation. We believe that when pH increased, the positive charge on the side chain was partially neutralized by  $\text{OH}^-$  ( $\text{R}_4\text{N}^+ + \text{OH}^- \leftrightarrow \text{R}_4\text{NOH}$ ). Consequently, the decreased charge density on polymer chain reduced the mutual repulsion among positive charges<sup>28–31</sup> and resulted in the planarization of the conjugated backbone. As pH continuously increased, the planarization of the conjugated backbone reached saturation and then the interchain aggregation was formed to retain the water-solubility of **P1'**.

The pH-influenced fluorescence intensity of **P1'** aqueous solution is described in Figure 4c. When pH < 7, the fluorescence intensity of **P1'** enhanced gradually and reached a plateau at about pH = 4.5. A previous study by Wrighton et al. showed that in comparison with alkoxy-substituted PPEs, the PPEs functionalized with tertiary amino group exhibited significantly lower PL intensity due to the interaction of the nonbonding electron pair on the nitrogen atom with the conjugated  $\pi$ -system which results in quenching of the excited state through intramolecular charge transfer.<sup>32</sup> Hence, the enhanced fluorescence intensity in an acidic environment can be attributed to the decreased interaction, by protonation, of those unquaternized tertiary amino group (55%) with the  $\pi$ -conjugated backbone. It is consistent with the higher fluorescence intensity of protonated amino-functionalized poly(*p*-phenylene)s than neutral amino-functionalized poly(*p*-phenylene)s reported by Reynolds et al.<sup>28</sup>

When pH > 7, the fluorescence intensity of **P1'** started to decrease swiftly at pH = 9.0 and arrived at the first



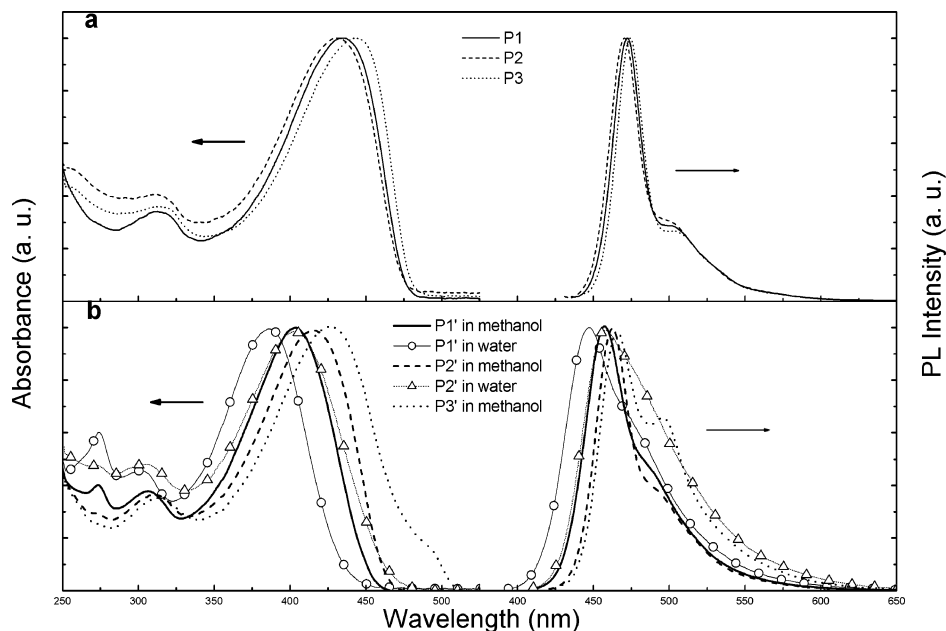


**Figure 3.** UV-vis absorption and PL emission spectra of (a) neutral polymers **P1**–**P3** in chloroform and (b) quaternized polymers **P1'**–**P3'** in water or methanol.

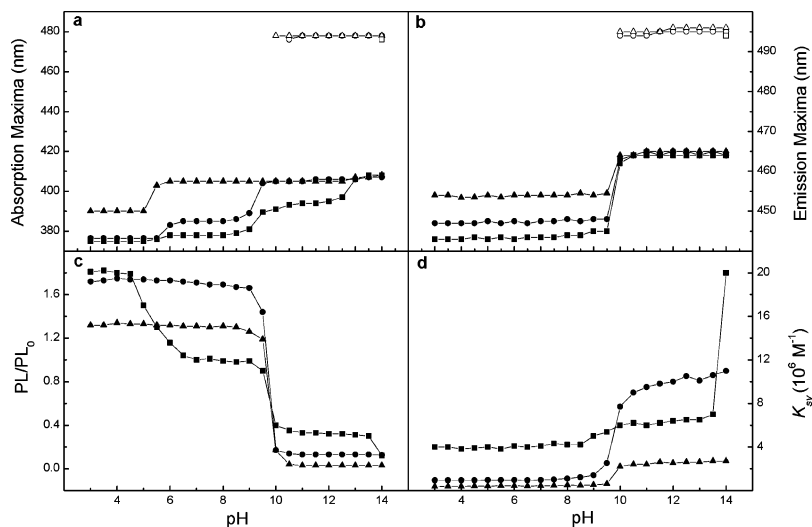


**Figure 4.** pH dependence of UV-vis absorption maxima, emission maxima, PL intensity, and fluorescence quenching by  $\text{Fe}(\text{CN})_6^{4-}$  of **P1'** in aqueous solution with various salt concentrations. Key: (—■—) [NaCl] = 0 M; (—●—) [NaCl] = 0.1 M; (—▲—) [NaCl] = 1 M. The new observable absorption and emission maxima: (—○—) [NaCl] = 0.1 M; (—△—) [NaCl] = 0.1 M. In Figure 4c, PL<sub>0</sub> refers to the fluorescence intensity of **P1'** aqueous solution at pH = 7 and [NaCl] = 0 M.

low point (0.4, compared with the pristine one at pH = 7) at about pH = 10. As we discussed previously, the planarization of the conjugated backbone, not interchain aggregation, formed in an alkaline environment at pH < 13. Thus, the general explanation that the reduced fluorescence intensity of anionic PPE in aqueous solution resulted from interchain aggregation<sup>22</sup> was not appropriate for our system. <sup>1</sup>H NMR spectra in Figure 2 show that the signal of unquaternized tertiary amino group of **P1'** shifted significantly to the lower field compared with that of tertiary amino group on its neutral analogue **P1**, and closed tightly to the signal of quaternized ammonium group of **P1'**. This indicates the reduced electron cloud density of the nonbonding electron pair on the nitrogen atom of unquaternized tertiary amino group under the positive-charge-rich environment. Thus, it was suggested that the neutralization of quaternized ammonium group by OH<sup>−</sup> in an alkaline environment reduced positive charge density, and hence-

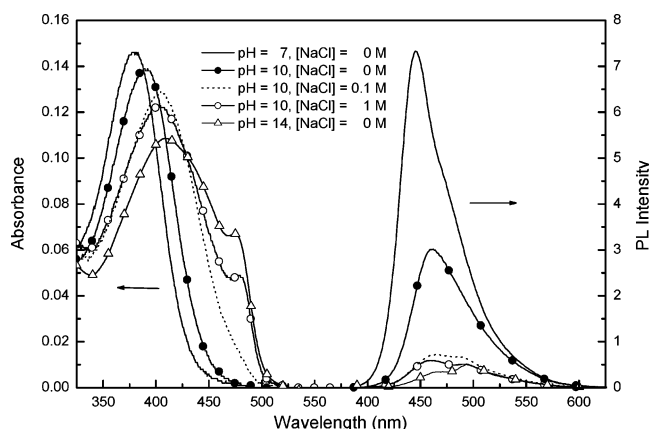
forth increased the activity of the unquaternized tertiary amino group, which led to its enhanced quenching ability on the conjugated backbone. When pH increased to 14, fluorescence intensity dramatically decreased to a new nadir (PL/PL<sub>0</sub> = 0.12), arising from the formation of interchain aggregation. Furthermore, the pH-influenced fluorescence intensity of **P1'** may be evident in fluorescence lifetime data (see Table 2). **P1'** showed a longer fluorescence lifetime ( $\tau$  = 0.57 ns) at pH = 4 than that at pH = 7 ( $\tau$  = 0.48 ns) while a shorter lifetime ( $\tau$  = 0.42 ns) at pH = 10; all of this is in accordance with the enhanced fluorescence intensity in an acidic environment and decreased fluorescence intensity in an alkaline environment and strongly indicated the existence of pH-dependent excited-state quenching.

The possible influence on the spectral changes of conjugated polymers by ionic strength has been studied by several researchers.<sup>3,36</sup> Herein, we studied the influence of ionic strength on the optical properties of **P1'**

**Table 2. Photophysical Properties and Fluorescence Quenching of P1' in Aqueous Solution with Different pH and Ionic Strength<sup>a</sup>**

pH	[NaCl]/M	absorption $\lambda_{\text{max}}/\text{nm}$	emission $\lambda_{\text{max}}/\text{nm}$	$\tau/\text{ns}$ at 450 nm (amplitude/%)	$\tau/\text{ns}$ at 500 nm (amplitude/%)	$K_{\text{sv}}/\text{M}^{-1}$
4	0.0	375	444	0.57 (100)	0.59 (100)	$3.8 \times 10^6$
	0.1	376	445	0.55 (100)	0.56 (100)	$9.4 \times 10^5$
	1.0	390	454	0.51 (100)	0.54 (100)	$3.8 \times 10^5$
7	0.0	378	444	0.48 (100)	0.50 (100)	$4.1 \times 10^6$
	0.1	385	445	0.53 (100)	0.56 (100)	$9.6 \times 10^5$
	1.0	405	454	0.50 (100)	0.52 (100)	$4.2 \times 10^5$
10	0.0	390	462	0.42 (100)	0.50 (100)	$6.0 \times 10^6$
	0.1	405	464, 494	0.40 (90), 5.46 (10)	0.55 (55), 5.80 (45)	$7.7 \times 10^6$
	1.0	405, 478	464, 494	0.39 (81), 4.76 (19)	0.49 (53), 5.32 (47)	$2.2 \times 10^6$
14	0.0	408, 476	464, 494	0.39 (79), 5.70 (21)	0.57 (48), 6.50 (52)	$2.0 \times 10^7$
	0.1	407, 478	464, 495	0.40 (75), 6.01 (25)	0.55 (45), 6.48 (55)	$1.1 \times 10^7$
	1.0	408, 478	465, 496	0.37 (73), 6.18 (27)	0.50 (45), 6.60 (55)	$2.7 \times 10^6$

<sup>a</sup> pH was adjusted with HCl and NaOH aqueous solutions at different concentrations ( $1$ ,  $1 \times 10^{-1}$  M,  $1 \times 10^{-2}$  M,  $1 \times 10^{-3}$  M,  $1 \times 10^{-4}$  M, and  $1 \times 10^{-5}$  M).

**Figure 5.** UV-vis absorption and PL emission spectra of P1' in aqueous solution with various pH and salt concentrations.

aqueous solution at different pH, which has never been investigated before. As shown in Figure 4, parts a and b, the absorption and emission maxima red shifted with the increase of ionic strength. It is noteworthy that when adding salts at pH = 7, the absorption maxima only red shifted to 405 nm and no new absorption and emission peak appeared at redder region, showing that adding salts at a neutral environment only leads to the planarization of P1' conjugated backbone. This result can be explained in terms of the effective screening of electrostatic repulsion<sup>3</sup> between positive ammonium groups by adding ions which led to the planarization of the conjugated backbone. However, when adding salts at pH  $\approx$  10, new absorption ( $\approx$ 478 nm) and emission ( $\approx$ 495 nm) maxima started to appear (see Figure 5). The redder absorption and emission maxima, close to that of P1' at pH = 14 belonging to interchain aggregation, strongly implied the formation of salt-assisted interchain aggregation for P1'. Time-resolved photoluminescent measurement showed that after adding salts at pH = 10, the fluorescence decay changed into biexponential and can be fitted to two components with  $\tau \approx$  0.4 and 5 ns (see Table 2). This observed new long lifetime emission decay component further confirmed the existence of interchain aggregation.<sup>10,22</sup> We have discussed previously that when pH increased to 10 the planarization of P1' backbone was formed. Thus, adding salts at pH = 10, the retained charge of P1' was screened and the hydrophilicity of P1' further decreased. Consequently, the polymer backbones tended to aggregate in order to optimize their hydrophobic properties and keep

the polymer chains soluble in water.<sup>10</sup> In addition, the planarization of P1' backbone induced by OH<sup>-</sup> and salts further afforded a good precondition for the formation of interchain  $\pi$ -aggregation.<sup>32</sup>

In conclusion, from Figure 4, it is visible that upon increasing pH or adding salts or both, the absorption and emission peak always initially red shifted and stopped at one position ( $\lambda_{\text{max}} \approx$  408 nm for UV and  $\lambda_{\text{max}} \approx$  464 nm for PL), and then a new peak appeared on a redder position ( $\lambda_{\text{max}} \approx$  478 nm for UV and  $\lambda_{\text{max}} \approx$  496 nm for PL). This clearly indicates that the pH- and salt-induced conformational change occurred from the planarization of the conjugated backbone to the interchain aggregation.

Interestingly, when NaCl solution was used as a fluorescence buffer solution for P1', the H<sup>+</sup>-induced fluorescence enhancement disappeared. The presented stable fluorescence intensity at pH  $\leq$  9 in buffer solution (see Figure 4c) made it very attractive in practical applications in a broader pH region. Besides, it was found that the fluorescence intensity first increased when [NaCl] = 0.01 M and then decreased when [NaCl] increased to 0.1 M. At present, we cannot explain those phenomena related to ionic strength while the influence from ionic strength on the quenching of conjugated backbone by nonbonding electron pair may exist. In contrast to the stable fluorescence intensity at pH  $\leq$  9, the fluorescence intensity of P1' decreased swiftly at pH = 10 after increasing ionic strength. Because of the formation of nonemissive decay channels at interchain aggregated state, we thus attribute the dramatic decrease of fluorescence intensity to the enhanced interchain aggregation at pH = 10.<sup>1</sup> In addition, the more extended  $\pi$ -conjugation obtained from the interchain aggregation may also be conducive to enhance the quenching ability of tertiary amino group on conjugated backbone, giving rise to more fluorescence quenching.<sup>22</sup>

**Stern-Volmer Study at Different pH.** One promising application of FWSCPs as highly sensitive chemosensors was found to be based on their rapid and collective response to relatively small perturbations in local environment.<sup>37</sup> A low concentration of quencher is sufficient to extinguish the fluorescence from the conjugated segments through electron transfer or energy transfer due to facile energy migration along the conjugated backbone, and relatively strong binding of the quencher with FWSCPs by electrostatic attraction. Therefore, to evaluate the amplified quenching effect of our water-soluble cationic PPE, the fluorescence



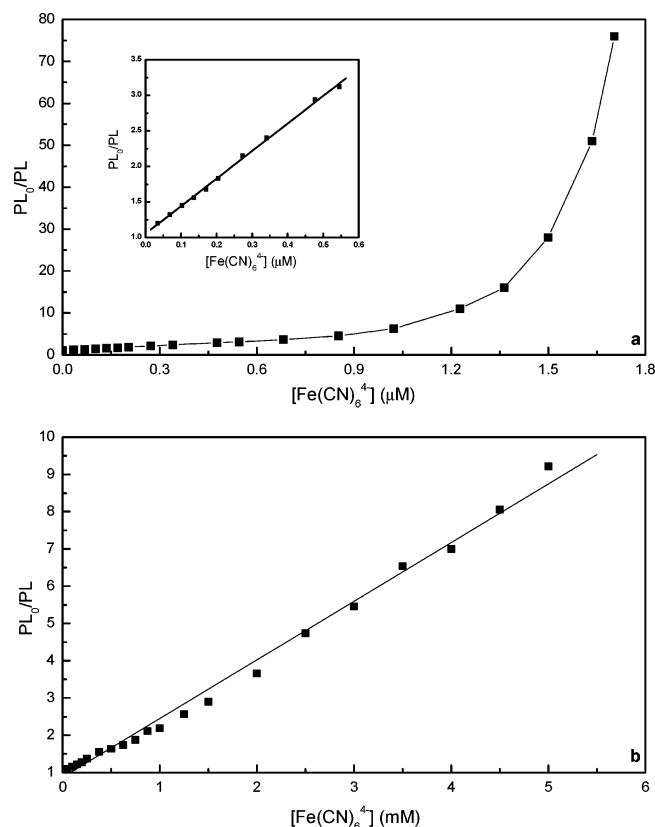


**Figure 6.** (a) Stern–Volmer plot of **P1'** quenched by  $\text{Fe}(\text{CN})_6^{4-}$  in aqueous solution at pH = 7 and  $[\text{NaCl}] = 0$  M. Inset: the part of Stern–Volmer plot of **P1'** quenched by  $\text{Fe}(\text{CN})_6^{4-}$  at low concentration. (b) Stern–Volmer plot of model compound **M1'** quenched by  $\text{Fe}(\text{CN})_6^{4-}$  in aqueous solution.

quenching of **P1'** by anionic quencher  $\text{Fe}(\text{CN})_6^{4-}$  was compared with its model compound **M1'**. Figure 6 showed the Stern–Volmer plots of **P1'** and **M1'** quenched by  $\text{Fe}(\text{CN})_6^{4-}$  in aqueous solution. As shown in Figure 6, **P1'** exhibited obviously amplified quenching that the quenching of **P1'** by anionic  $\text{Fe}(\text{CN})_6^{4-}$  ( $K_{\text{sv}} = 4.1 \times 10^6 \text{ M}^{-1}$ ) is three orders more efficient than its model compound **M1'** ( $K_{\text{sv}} = 1.3 \times 10^3 \text{ M}^{-1}$ ) due to the high delocalization of singlet exciton and the rapidness of the energy migration along the conjugated backbone of **P1'**.<sup>1,21a,21b</sup> The upward Stern–Volmer curve which was observed for the fluorescence quenching of **P1'** is different from the straight line for **M1'**. This significant difference can be explained by the existence of sphere-of-action for polymer chain in aqueous solution,<sup>3</sup> which could be described by the modified Stern–Volmer equation:

$$\frac{F_0}{F} = (1 + K_{\text{sv}}^{\text{S}}[Q])$$

unmodified Stern–Volmer equation  
(straight line)<sup>38</sup>

$$\frac{F_0}{F} = (1 + K_{\text{sv}}^{\text{S}}[Q])e^{\alpha V[Q]}$$

modified Stern–Volmer equation (upward curve)

where  $F_0$  is the fluorescence intensity,  $F$  is the fluorescence intensity,  $[Q]$  is the quencher concentration,  $K_{\text{sv}}$  is the Stern–Volmer constant,  $V$  is the volume constant, and  $\alpha$  is used to account for the charge-induced enhancement of the local quencher concentration.

The  $K_{\text{sv}}$  of **P1'** vs pH was depicted in Figure 4d. When  $\text{pH} < 7$ , although the fluorescence intensity was enhanced,  $K_{\text{sv}}$  was nearly unchanged, indicating that the addition of  $\text{H}^+$  hardly influenced the quenching efficiency of **P1'**. However, the  $K_{\text{sv}}$  slightly increased in an alkaline environment at  $\text{pH} < 13$ . Recent studies have reported that conjugated polymers have more amplified quenching than conjugated oligomer, because their extended  $\pi$ -aggregation enhanced the delocalization of singlet exciton and the rapidness of the energy migration.<sup>1</sup> Thus, we suggest that the amplified quenching efficiency result from the  $\text{OH}^-$ -induced extended conjugated length. After adding salts at  $\text{pH} = 7$ ,  $K_{\text{sv}}$  decreased with the increase of ionic strength (see Table 2). This result is consistent with the notion that add ions will screen the electrostatic attraction between conjugated polyelectrolyte and quencher with counterions and remove quencher from the vicinity of conjugated polyelectrolyte and finally decrease the  $K_{\text{sv}}$ . Adding salts at  $\text{pH} = 10$  or increasing pH to 14 resulted in a more enhanced quenching ability, which can be explained by the formed interchain aggregation that could lead to further amplification of fluorescence quenching through the occurring of interchain exciton migration.<sup>1,22</sup>

## Conclusions

In summary, we report on the successful syntheses of a series of cationic PPEs. **P1'**, prepared through quaternization of the neutral PPE with tertiary amino group in all side chains, exhibits intrinsic water-solubility compared with other cationic PPEs **P2'** and **P3'** containing side chains with different hydrophilicity. Interchain aggregation was observed for **P3'** in methanol, which may result from the presence of long chain hydrophobic groups. Study on the variation of the absorption and emission spectra of **P1'** in aqueous solution with pH exhibits that with pH increase, the planarization of the conjugated backbone is first formed before the formation of interchain aggregation. Besides, the pH-influenced fluorescence intensity of **P1'** was also found and explained by pH-influenced quenching of  $\pi$ -conjugated backbone by unquaternized tertiary amino group. Such a pH-influenced fluorescence intensity can be efficiently buffered by adding salts at  $\text{pH} < 10$ . Although adding salts in a neutral environment only creates the planarization of **P1'** conjugated backbone, adding salts in an alkaline environment significantly promotes the formation of interchain aggregation. The investigation of fluorescence quenching of **P1'** by  $\text{Fe}(\text{CN})_6^{4-}$  exhibits that such a water-soluble cationic PPE possesses amplified sensitivity on anionic quencher. In addition, its  $K_{\text{sv}}$  highly increased in an alkaline environment due to the elongated  $\pi$ -conjugation from the planarization of conjugated backbone and the interchain aggregation.

**Acknowledgment.** This work was financially supported by the National Natural Science Foundation of China under Grants 60325412, 90406021, and 50428303 as well as the Shanghai Commission of Science and Technology under Grants 022261042, 03DZ11016, and 04XD14002 and the Shanghai Commission of Education under Grant 2003SG03.

## References and Notes

- (1) Chen, L.; McBranch, D. W.; Wang, H.-L.; Helgeson, R.; Wudl, F.; Whitten, D. G. *Proc. Natl. Acad. Sci. U.S.A.* **1999**, *96*, 12287.

- (2) Gaylord, B. S.; Heeger, A. J.; Bazan, G. C. *Proc. Natl. Acad. Sci. U.S.A.* **2002**, *99*, 10954.
- (3) Wang, J.; Wang, D. L.; Miller, E. K.; Moses, D.; Bazan, G. C.; Heeger, A. J. *Macromolecules* **2000**, *33*, 5153.
- (4) Wang, D. L.; Wang, J.; Moses, D.; Bazan, G. C.; Heeger, A. J. *Langmuir* **2001**, *17*, 1262.
- (5) Chen, L.; McBranch, D.; Wang, R.; Whitten, D. G. *Chem. Phys. Lett.* **2000**, *330*, 27.
- (6) Chen, L.; Xu, S.; McBranch, D.; Whitten, D. G. *J. Am. Chem. Soc.* **2000**, *122*, 9302.
- (7) Jones, R. M.; Bergstedt, T. S.; McBranch, D. W.; Whitten, D. G. *J. Am. Chem. Soc.* **2001**, *123*, 6726.
- (8) Stork, M.; Gaylord, B. S.; Heeger, A. J.; Bazan, G. C. *Adv. Mater.* **2002**, *14*, 361.
- (9) Fan, C.; Plaxco, K. W.; Heeger, A. J. *J. Am. Chem. Soc.* **2002**, *124*, 5642.
- (10) Pinto, M. R.; Kristal, B. M.; Schanze, K. S. *Langmuir* **2003**, *19*, 6523.
- (11) Pinto, M. R.; Schanze, K. S. *Synthesis* **2002**, *9*, 1293.
- (12) Wang, D.; Gong, X.; Heeger, P. S.; Rininsland, F.; Bazan, G. C.; Heeger, A. J. *Proc. Natl. Acad. Sci. U.S.A.* **2002**, *99*, 49.
- (13) Gaylord, B. S.; Wang, S.; Heeger, A. J.; Bazan, G. C. *J. Am. Chem. Soc.* **2001**, *123*, 6417.
- (14) Hong, J. W.; Gaylord, B. S.; Bazan, G. C. *J. Am. Chem. Soc.* **2002**, *124*, 11868.
- (15) Harrison, B. S.; Ramey, M. B.; Reynolds, J. R.; Schanze, K. S. *J. Am. Chem. Soc.* **2000**, *122*, 8561.
- (16) Gaylord, B. S.; Heeger, A. J.; Bazan, G. C. *J. Am. Chem. Soc.* **2003**, *125*, 896.
- (17) Liu, B.; Gaylord, B. S.; Wang, S.; Bazan, G. C. *J. Am. Chem. Soc.* **2003**, *125*, 6705.
- (18) Wang, S.; Liu, B.; Gaylord, B. S.; Bazan, G. C. *Adv. Funct. Mater.* **2003**, *13*, 463.
- (19) Liu, B.; Wang, S.; Bazan, G. C.; Mikhailovsky, A. J. *J. Am. Chem. Soc.* **2003**, *125*, 13306.
- (20) Bunz, U. H. F. *Chem. Rev.* **2000**, *100*, 1605.
- (21) (a) Zhou, Q.; Swager, T. M. *J. Am. Chem. Soc.* **1995**, *117*, 7017. (b) Zhou, Q.; Swager, T. M. *J. Am. Chem. Soc.* **1995**, *117*, 12593. (c) Yang, J.-S.; Swager, T. M. *J. Am. Chem. Soc.* **1998**, *120*, 5321. (d) Yang, J.-S.; Swager, T. M. *J. Am. Chem. Soc.* **1998**, *120*, 11864. (e) Kim, J.; McQuade, D. T.; McHugh, S. K.; Swager, T. M. *Angew. Chem., Int. Ed.* **2000**, *39*, 3869.
- (22) Tan, C.; Pinto, M. R.; Schanze, K. S. *Chem. Commun.* **2002**, 446.
- (23) Thünemann, A. F. *Langmuir* **2001**, *17*, 5098.
- (24) DiCesare, N.; Pinto, M. R.; Schanze, K. S.; Lakowicz, J. R. *Langmuir* **2002**, *18*, 7785.
- (25) Kushon, S. A.; Ley, K. D.; Bradford, K.; Jones, R. M.; McBranch, D.; Whitten, D. *Langmuir* **2002**, *18*, 7245.
- (26) McQuade, D. T.; Hegedus, A. H.; Swager, T. M. *J. Am. Chem. Soc.* **2000**, *122*, 12389.
- (27) Koishi, K.; Ikeda, T.; Kondo, K.; Sakaguchi, T.; Kamada, K.; Tawa, K.; Ohta, K. *Macromol. Chem. Phys.* **2000**, *201*, 525.
- (28) Balanda, P. B.; Ramey, M. B.; Reynolds, J. R. *Macromolecules* **1999**, *32*, 3970.
- (29) Liu, B.; Yu, W.; Lai, Y. H.; Huang, W. *Chem. Commun.* **2000**, 551.
- (30) Liu, B.; Yu, W.; Lai, Y. H.; Huang, W. *Macromolecules* **2002**, *35*, 4975.
- (31) Fan, Q.-L.; Lu, S.; Lai, Y.-H.; Huang, W. *Macromolecules* **2003**, *36*, 6976.
- (32) Weder, C.; Wrighton, M. S. *Macromolecules* **1996**, *29*, 5157.
- (33) Kim, J.; Swager, T. M. *Nature (London)* **2001**, *411*, 1030.
- (34) McCullough, R. D.; Ewbank, P. C.; Loewe, R. S. *J. Am. Chem. Soc.* **1997**, *119*, 633.
- (35) Levitus, M.; Schmieder, K.; Ricks, H.; Schimizu, K. D.; Bunz, U. H. F.; Garcia-Garibay, M. A. *J. Am. Chem. Soc.* **2001**, *123*, 4259.
- (36) Kim, B.-S.; Chen, L.; Gong, J.; Osada, Y. *Macromolecules* **1999**, *32*, 3964.
- (37) McQuade, D. T.; Pullen, A. E.; Swager, T. M. *Chem. Rev.* **2000**, *100*, 2537.
- (38) Lakowicz, J. R. In *Principles of Fluorescence Spectroscopy*, 2nd ed.; Plenum Press: New York, 1999.

MA048717K